PHOTOCATALYTIC REMOVAL OF PHENOL USING TITANIUM DIOXIDE (TiO_2) IN FLUIDIZED BED REACTOR

BY

TAN YONG NIAN

Thesis submitted in fulfillment of the

degree of

Master of Science

2012

ACKNOWLEGEMENTS

I would like to express my sincere gratitude to my supervisor, Professor Abdul Rahman Mohamed for his guidance, supports, advices, and ideas throughout my research study.

I would also like to thank all the lecturers, staffs, and technicians in School of Chemical Engineering, Universiti Sains Malaysia (USM). I would like to acknowledge the technicians of School of Material and Mineral Resources Engineering and School of Biology Science for the help in sample analyzing. Furthermore, I would like to thank all my friends for their kindness and their help during my research.

I would also like to take this opportunity to thank the financial supports received from USM through the USM Fellowship, Fundamental Research University Grant Scheme (No. 811068), and Postgraduate Research Grant Scheme (USM-RU-PRGS No. 8033051).

Lastly, I would like to thank my parents and family with their encouragement and support through my research life.

TABLE OF CONTENTS

LIST OF TABLES

LIST OF FIGURES

LIST OF SYMBOLS

Symbol	Description	Unit
Ag	Silver atom	-
Ba	Barium atom	-
Br	Bromine atom	-
Br^-	Bromide ions	-
C	Carbon atom	-
C	Concentration of substrate	mg/L
C_6H_5OH	Phenol	-
C_0	Initial pollutant concentration	mg/L
C_p	Concentration of phenol	mg/L
C_t	Concentration of phenol at reaction time, t	mg/L
Ca^{2+}	Calcium (II) ions	-
$CaCl_2$	Calcium chloride	-
Ce	Cerium atom	-
$Ce(NO_3)_4$	Cerium (IV) nitrate	-
$CH_3CH_2NH_2$	Ethylamine	-
Cl^-	Chloride ions	-
CO_3^{2-}	Carbonate ions	-
Co	Cobalt atom	-
Co^{2+}	Cobalt (II) ions	-
Cr	Chromium atom	-
Cr^{3+}	Chromium (III) ions	-
$CS(NH_2)_2$	Thiourea thiocarbamide	-
Cu	Copper atom	-

Symbol	Description	Unit
Cu^{2+}	Cooper (II) ions	-
D	Crystallite size	nm
F	Fluorine atom	-
F^-	Fluoride ions	-
Fe	Iron atom	-
Fe^{3+}	Iron (III) ions	-
$FeCl_2$	Iron (II) chloride	-
$FeCl_3$	Iron (III) chloride	-
$Fe(NO_3)_3$	Iron (III) nitrate	-
HCO_3^-	Bicarbonate ions	-
H_2O_2	Hydrogen peroxide	-
H_2O	Water molecules	-
HO•	Hydroxyl radicals	-
H_3PO_2	Hypophosphorous acid	
H_3PO_4	Phosphoric acid	-
H_2PtCl_6	Chloroplatinic acid hexahydrate	-
I	Iodine atom	-
k_{app}	Apparent reaction rate constant	1/min
K	Adsorption coefficient	L/mg
K^+	Potassium ions	-
K_{Sch}	Scherrer constant	-
KCl	Potassium chloride	-
Mg^{2+}	Magnesium ions	-
Mn	Manganese atom	-

Symbol	Description	Unit
n	Number of independent variables	-
N	Nitrogen atom	-
$NaHCO_3$	Sodium bicarbonate	-
$NaNO_3$	Sodium nitrate	-
Na_2SO_4	Sodium sulphate	-
NH_4F	Ammonium fluoride	-
Ni	Nickel atom	-
Ni^{2+}	Nickel (II) ions	-
NO_3^-	Nitrate ions	-
O_2	Oxygen	-
$O_2^{\bullet -}$	Superoxide radical anion	-
O_3	Ozone	-
-OH	Hydroxide group	-
P	Phosphorus atom	-
Pd	Palladium atom	-
pH	Measure of the acidity or basicity of an aqueous solution	-
PO_4^-	Phosphate ions	-
Pt	Platinum atom	-
$PtCl_2$	Platinum (II) chloride	-
r	Rate of photocatalytic degradation of phenol	mg/L.min
r/r	Molar ratio	-
R_{ads}	Adsorbed pollutant	-
R_F	Ti:F molar ratio	-
Ru	Ruthenium	-

Symbol	Description	Unit
S	Sulphur	-
SO_4^{2-}	Sulphate ions	-
t	Time	h
$TiCl_3$	Titanium (III) chloride	-
$TiCl_4$	Titanium (IV) chloride	-
TiO_2	Titanium dioxide	-
$Ti(OBu)_4$	Titanium tetra-butoxide	-
$(Ti(OC_4H_{9-n})_4$	Tetra-butyl titanate	-
$Ti(OPr^i)_4$	Titanium tetra-isopropoxide	-
$Ti(SO_4)_2$	Titanium (IV) sulphate	-
TiS_2	Titanium sulphide	-
V	Vanadium atom	-
$VO(OPr)_3$	Vanadium alkoxides	-
x	Independent variables	-
X_1	Catalyst loading	mg/L
X_2	Air flow rate	L/h
X_3	Initial phenol concentration	mg/L
Zn	Zinc atom	-
Zn^{2+}	Zinc (II) ions	-
$ZnCl_2$	Zinc chloride	-

Greek Symbols

Symbol	Description	Unit
α	Rotatability	-
≡	Electron bonds	-
θ	Bragg's angle	°
λ	X-ray wavelength	nm
β_d	Half angular width at highest intensity diffraction peak	°

LIST OF ABBREVIATIONS

AC	Activated carbon
ANOVA	Analysis of variance
AOP	Advanced oxidation process
BET	Brunauer-Emmett-Teller
BJH	Barrett-Joyner-Halenda
CCC	Central composite circumscribed
CCD	Central composite design
CCF	Central composite face-centred
CCI	Central composite inscribed
COD	Chemical oxygen demand
DF	Degree of freedom
DIOX	1, 4-dioxane
DOE	Design of experiment
EDTA	Ethylenediaminetetraacetic acid
EDX	Energy dispersive X-ray spectroscopy
HPLC	High performance liquid chromatography
pzc	Point of zero charge
RSM	Response surface methodology
SEM	Scanning electron microscopy
SNTZS	Supported nano-TiO_2/ZSM-5/silica gel
TBOT	Titanium tetra-butoxide
TEA	Triethanolamine
TEM	Transmission electron microscopy
TNBT	*Titanium*(IV) n-butoxide

TOC	Total organic carbon
TTB	Titanium tetra-butoxide
TTIP	Tetra-titanium iso-propoxide
USEPA	US environmental protection agency
UV	Ultraviolet
VOCs	Volatile organic compounds

PENYINGKIRAN PEMFOTOMANGKINAN FENOL DENGAN MENGGUNAKAN TITANIUM DIOKSIDA (TiO_2) DALAM REAKTOR LAPISAN TERBENDALIR

ABSTRAK

Fluorin titanium dioksida (F-TiO_2) dan F-TiO_2 yang tersekat gerak telah disintensiskan oleh kaedah kombinasi sonikasi dan hidroterma serta kaedah pengikatan. Tambahan anion fluorin, tersekat gerak TiO_2, kaedah hidroterma dengan reaktor lapisan terbendalir digunakan dalam pemfotomangkinan degradasi fenol. Sampel telah dikaji dengan menggunakan pembelauan sinar-X (XRD), kaedah Brunauer-Emmett-Teller (BET), mikroskop elektron pengimbasan (SEM), penyebaran elektron sinar-X (EDX), dan mikroskop elektron transmisi (TEM). Penyingkiran pemfotomangkinan fenol telah diselidik di bawah sinaran cahaya ultraungu dalam reaktor lapisan terbendalir dengan menggunakan fotomangkin yang disediakan. Berdasarkan hasil pencirian XRD, semua pembelauan puncak fotomangkin F-TiO_2 adalah berhubungan kepada fasa anatis - TiO_2. Morfologi permukaan F-TiO_2 yang dihasilkan pada Ti:F nisbah molar 0.15 dan tempoh hidroterma selama 10 jam menunjukkan penyebaran partikel yang seragam apabila dikesan oleh kedua-dua analisis SEM dan TEM. Nilai tertinggi bagi luas permukaan BET, jumlah isipadu liang, dan saiz purata liang F-TiO_2 telah dinotiskan di Ti:F nisbah molar (R_F) 0.15 dan tempoh hidroterma 10 jam. Kewujudan F, Ti dan O pada permukaan F-TiO_2 telah disahkan oleh kajian EDX. Komposisi optimum fotomangkin yang terdiri daripada F-TiO_2, pasir kuarsa, dan silika koloid adalah

1:1.5:1. Berdasarkan imej TEM, F-TiO_2 disediakan pada Ti:F nisbah molar 0.15 di bawah tempoh hidroterma 10 jam (8.4 nm) mempunyai saiz kristal yang agak kecil berbanding dengan F-TiO_2 yang tersekat gerak (45-60 nm). F-TiO_2 yang dihasilkan pada Ti:F nisbah molar 0.15 bagi tempoh hidroterma 10 jam menunjukkan kadar penyingkiran fenol tertinggi. Keputusan untuk pembolehubah proses yang dikaji adalah: muatan pemangkin yang optimum adalah didapati 4 g/L; kepekatan fenol awal yang optimum adalah diperhatikan 20 mg/L; kadar aliran udara memberi nilai optimum 2 L/min; kation logam menghalang aktiviti pemfotomangkinan fotomangkin dalam susunan $K^+ > Ca^{2+} > Zn^{2+}$; anion tak organik juga menghalang tindak balas pemfotomangkinan dalam turutan $SO_4^{2-} > HCO_3^- > NO_3^-$. F-$TiO_2$ yang tersekat gerak memberikan prestasi degradasi pemfotomangkinan yang lebih baik berbanding dengan TiO_2 komersial Degussa P25. Degradasi pemfotomangkinan fenol didapati mematuhi tindak balas tertib pertama dengan nilai pemalar kadar, *k* sama dengan 2.19 mg/L.min dan nilai pemalar jerapan, K sama dengan 0.0305 L/mg, masing-masing. Rekabentuk ujikaji metodologi permukaan sambutan (RSM) berdasarkan kepada reka bentuk gabungan berpusat (CCD) telah digunakan untuk mengkaji dan mengoptimum interaksi kesan ke atas degradasi pemfotomangkinan fenol dengan menggunakan F-TiO_2 yang tersekat gerak. Degradasi pemfotomangkinan fenol yang optimum telah dicapai dalam 105 minit dengan muatan pemangkin sebanyak 4 g/L, kadar aliran udara sebanyak 2 L/min, dan kepekatan fenol awal sebanyak 20 mg/L.

PHOTOCATALYTIC REMOVAL OF PHENOL USING TITANIUM DIOXIDE (TiO_2) IN FLUIDIZED BED REACTOR

ABSTRACT

Fluorinated titanium dioxide (F-TiO_2) and immobilized F-TiO_2 were synthesized by sonication-hydrothermal method and binding method. Fluorine doping, immobilization, hydrothermal method and fluidized bed reactor used in this study. The samples were characterized by X-ray diffraction (XRD), Brunauer-Emmett-Teller (BET) analysis, scanning electron microscopy (SEM), energy dispersive X-ray spectroscopy (EDX), and transmission electron microscopy (TEM). The photocatalytic degradation of phenol using the prepared photocatalyst was evaluated under UV light irradiation in batch mode fluidized bed reactor. Based on the XRD patterns, all the diffraction peaks of the F-TiO_2 photocatalysts corresponded to the anatase phase of TiO_2. The surface morphology of F-TiO_2 observed by both SEM and TEM was uniformly distributed and the largest of BET surface area, total pore volume, and average pore size of F-TiO_2 at the Ti:F molar ratio of 0.15 under hydrothermal duration of 10 h. The presence of F, Ti, and O on the surface of F-TiO_2 was confirmed by EDX analysis. The optimum composition of the photocatalyst comprising F-TiO_2, quartz sand, and colloidal silica was 1:1.5:1. Based on TEM images, F-TiO_2 prepared in the Ti:F molar ratio of 0.15 under hydrothermal duration of 10 hours (8.4 nm) had a relatively smaller crystalline size compared to the supported F-TiO_2 (45-60 nm). F-TiO_2 produced at the Ti:F molar ratio of 0.15 for hydrothermal duration of 10 h showed the highest degradation rate of phenol. The

results for the studied operating parameters were: the optimal catalyst loading was found to be 4 g/L; the optimum initial phenol concentration was observed to be 20 mg/L; the air flow rate gave an optimum value of 2 L/min; the presence of metal cations impeded the photocatalytic activity of photocatalyst in the order of K^+ > Ca^{2+} > Zn^{2+}; the addition of inorganic anions also inhibited the photocatalytic reaction in the order of SO_4^{2-} > HCO_3^- > NO_3^-. Immobilized F-TiO_2 gave the better photocatalytic activity as compared to commercial Degussa TiO_2 P25. The photocatalytic degradation of phenol fitted well with pseudo first order kinetic model with its reaction rate constant, *k* equal to 2.19 mg/L.min and the adsorption constant, *K* equal to 0.0305 L/mg, respectively. Response surface methodology (RSM) based on the central composite design (CCD) used to optimize the photocatalytic degradation of phenol. The optimum phenol photodegradation was achieved in 105 minutes at the catalyst loading of 4 g/L, air flow rate of 2 L/min, and initial phenol concentration of 20 mg/L.

CHAPTER 1

INTRODUCTION

1.1 Treatment of Industrial Effluent

Water pollution is becoming a chronic global issue nowadays. Based on World Water Development Report (WWDR), in many developing countries, industries contribute around 22 % of the total world water usage and around 70 % of untreated industrial wastes are simply discarded into wastewater without prior filtering or processing (WWDR, 2011). The world faces enormous challenges ahead as drinkable water runs short due to natural disasters, population increase and water pollutions. Meanwhile, inappropriate treatment of hazardous and toxic organic pollutants in the wastewater could bring adverse effects to aquatic life and mammalian.

In Malaysia, Environmental Quality Act 1974 was implemented to prevent, abate, control the pollution and enhance the environment conditions. The Environmental Quality Act 1974 has set a limit of 0.2 mg/L of phenol in the discharged waste streams. To address these problems, advanced oxidation processes (AOPs) have been focused on current research to provide an environmentally benign and low cost approach for the treatment of organic pollutants before it is discharged to the receiving environment. In AOPs, highly reactive radicals are generated to treat and degrade the toxic and non-degradable pollutants in the wastewater efficiently without involving complex technologies and contributing secondary pollutions.

1.2 Heterogeneous Photocatalysis

Advanced oxidation processes (AOPs) have been applied in the wastewater treatment to degrade, oxidize, and mineralize the organic pollutants which are resistant to be removed or mineralized by conventional techniques. Heterogeneous photocatalysis is useful for the treatment of wastewater containing toxic and carcinogenic pollutants such as colouring compounds, aromatics, and volatile organic compounds. In general, heterogeneous photocatalysis have been applied to generate highly reactive oxidant species such as hydroxyl radicals by combining oxygen (O_2) and ultraviolet (UV) irradiation on the surface of photocatalyst. The hydroxyl radical (HO•) is a strong and powerful oxidant, which acts very rapidly with those toxic pollutants. Those pollutants are chemically transformed and completely mineralized to harmless products such as carbon dioxide and water (Brillas *et al.,* 1998).

Titanium dioxide (TiO_2) has been used in heterogeneous photocatalysis due to its several unique characteristics. TiO_2 is an ideal photocatalyst due to its intrinsic properties such as chemically stable, widespread availability, cheap, non-toxic, and wide band gap (Fujishima *et al.*, 2007). TiO_2 photocatalyst is also proven as an excellent compound to have double aptitude characteristic, which can absorb reactants and photons simultaneously (Hermann *et al.,* 2007). The heterogeneous photocatalysis can be carried out effectively to degrade and mineralize organic pollutants in gas or liquid phases using TiO_2 photocatalysts (Augugliaro *et al.,* 2006).

Otherwise, considerable attempts have been carried out in the development of TiO_2 photocatalysts for environmental protection procedures such as metal ions reduction, antibacterial protection, treatment of harmful gas emission, and hazardous waste remediation (Addamo *et al.,* 2005; Hermann *et al.,* 2007). TiO_2 has been

improved and developed for the high percentage of degradation of organic and inorganic pollutants in the present day photocatalytic oxidation technology (Addamo *et al.,* 2005).

1.3 Problem Statement

TiO_2 is an effective photocatalyst in many environmental protection procedures especially in the treatment of organic pollutants. However, there are some limitations for its wide practical application in photocatalysis, which are thermal instability (Zhang *et al.*, 2009a), incompatibility of the hydrophilic TiO_2 to interact with hydrophobic organic pollutants such as phenol, and the tendency for spontaneous loss of the electron-hole through their recombination with free electrons, thereby dissipating their capacity for photocatalysis (Shaban and Khan, 2008; Zhu *et al.,* 2008). Hence, various modified presentations of TiO_2, such as doping techniques with various metal or non-metal dopants have been attempted in order to increase the pollutant degradation efficiency of the TiO_2 photocatalyst. Basically, doping techniques can be used to improve the physical properties of TiO_2. Cai *et al.* (2008) reported that suitable amounts of dopants have been applied in the formation of photocatalysts in order to produce high specific surface area and excellent morphology and crystallite size of TiO_2. An optimum rate of doping also prevents the transformation of the anatase phase to the rutile phase.

Doping TiO_2 with fluoride anions (F^-) has been investigated in this research with the aim at inhibiting the recombination rate of holes and free electrons. ≡Ti-F groups of fluorinated TiO_2 (F-TiO_2) are reported to trap the photogenerated electrons by transferring the electrons to O_2 on the surface of F-TiO_2 (Yu *et al.*, 2009a). At the same time, doping TiO_2 with fluoride anions promotes the formation of the anatase

phase of the photocatalyst. The hydrophobic nature of fluoride anions increases the affinity of TiO_2 towards the organic pollutants such as phenol due to the replacement of the ≡OH group by the F^- ion. The photocatalytic performance of the fluorinated TiO_2 photocatalysts is then improved with these excellent present properties.

There are two types of TiO_2 were studied in the photocatalysis, which are TiO_2 suspended in aqueous medium and TiO_2 immobilized on supports (Gumy *et al.,* 2006; Zhang *et al.*, 2008). However, there are some disadvantages found in the suspended TiO_2 photocatalysts such as UV light scattering by TiO_2 particles causing the reduction of UV light penetration to TiO_2 surface and difficulty in filtering out the ultrafine TiO_2 particle after photocatalytic degradation process (Lee *et al.*, 2002; Mascolo *et al.*, 2007). The problems can be overcame by immobilization of TiO_2 with various supports, such as, silica (Uchiyama *et al.*, 2005), glass tube (Ryu *et al.*, 2003), and activated carbon (Sun *et al.*, 2009). Quartz sand was chosen as support due to its transparency, chemically inert, high surface area, and strong adsorption affinity. Synthesis of immobilized TiO_2 is important to improve the photocatalytic degradation reaction associated with immobilization process owing to its high surface area. In addition, the strong adsorptive capacity of the supported catalysts can be investigated in achieving complete mineralization of organic pollutants at a much lower power consumption compared to suspended TiO_2 (Li *et al.*, 2007). The knowledge especially in the immobilization of TiO_2 still requires better understanding.

As most commonly known, various methods like sol-gel (Keshmiri *et al.*, 2006) and chemical vapour deposition (Kim *et al.*, 2008), are popular techniques for the synthesis of nano-TiO_2. However, these methods are not commercially viable for the large scale production because they are inflexible and ineffective as compared to

hydrothermal method. In addition, they are time consuming and complicated compared to hydrothermal method; for example, further calcination process is required for sol gel method to induce the crystallization process (Keshmiri *et al.*, 2006). Meanwhile, hydrothermal method could produce highly crystallite anatase TiO_2 nanoparticles at elevated temperature (Seo *et al.*, 2010). In this work, a systematic and detailed procedure to synthesize a well-crystalline, uniform, and dispersed fluorinated TiO_2 is required to investigate and improve its photocatalytic activity and efficiency to remove aqueous phenol solution.

Reactor is one of the important criteria in photocatalytic degradation process as it plays a role for the photocatalyst to react with pollutant. There are several types of reactors utilizing nano-TiO_2 photocatalysts have been developed in the photocatalysis and the reactors can be classified into 3 categories: slurry reactor using suspended TiO_2, immobilized TiO_2 in fixed bed reactor, and immobilized TiO_2 in fluidized bed reactor (Ngah, 2005). An efficient reactor should possess certain criteria such as: efficient UV light irradiation, excellent reactant contact, high photocatalyst loading, good mixing condition, and efficient heat and mass transfer (Chiovetta *et al.*, 2001; Nemtsov and Zababniotou, 2008). A fluidized bed reactor is chosen in this study where intimate contact of photocatalyst, UV light, and aqueous phenol solution can be achieved (Ramesh *et al.*, 2009). However, the technical development is still under investigation in the photocatalytic degradation reaction. Thus, a detailed study on the effect of process parameters such as catalyst loading, initial phenol concentration, air flow rate, etc. is carried out to optimize the reaction performance of the prepared photocatalyst in pollutant degradation. The importance of the present work is to exploit the wide and ever-growing application of photocatalysts to be more practical in the wastewater treatment by studying the

factors in the synthesis of fluorinated TiO_2 and supported fluorinated TiO_2 with their photocatalytic performance in a fluidized bed reactor.

1.4 Research Objectives

The main aim of this project is to produce fluorinated titanium dioxide (F-TiO_2) with high photoactivity to degrade phenol in water under UV irradiation. The objectives of this project are listed as follow:

1) To synthesize fluorinated TiO_2 by hydrothermal method and immobilize the prepared fluorinated TiO_2 on quartz sand using simple binding method.
2) To characterize the physical properties of fluorinated TiO_2 and immobilized F-TiO_2 using transmission electron microscopy (TEM), scanning electron microscopy (SEM), energy dispersive X-ray spectroscopy (EDX), X-ray diffractometer (XRD), and the Brunauer-Emmett-Teller (BET) technique.
3) To study the performance of the prepared photocatalyst on the photocatalytic degradation of phenol in the fluidized batch reactor. The operating parameters such as catalysts loading, initial phenol concentration, air flow rate, inorganic anions, and metal cations were investigated on the photocatalytic degradation of phenol using immobilized F-TiO_2 in fluidized bed reactor.
4) To study the kinetics of photocatalytic degradation of phenol using immobilized F-TiO_2 based on Langmuir Hinshelwood kinetics model.

1.5 Scope of Study

The production of immobilized F-TiO_2 with high photocatalytic activity is the main scope in this project. In this project, hydrothermal method was chosen to

synthesize the F-TiO_2 photocatalysts by varying two synthesis parameters: hydrothermal treatment duration and amount of fluoride doped. The characterizations of F-TiO_2 photocatalyst were carried out using scanning electron microscopy (SEM), X-ray diffraction (XRD), Brunauer-Emmett- Teller (BET) technique, energy dispersive X-ray microscope spectroscopy (EDX), and transmission electron (TEM). The photocatalytic degradation performance of photocatalysts was evaluated through the photocatalytic degradation of aqueous phenol solution in a fluidized bed reactor.

Next, F-TiO_2 produced was further immobilized on quartz sand using a simple binding method. The characterizations of F-TiO_2 photocatalyst were carried out using transmission electron microscope (TEM). Fluidized bed reactor was used to degrade the aqueous phenol solution using immobilized F-TiO_2 produced. Various process parameters such as catalyst loading (1 g/L-5 g/L), initial phenol concentration (10 mg/L-50 mg/L), metal cations (Zn^{2+}, Ca^{2+}, and K^+ ions), inorganic anions (SO_4^{2-}, HCO_3^-, NO_3^- ions), and air flow rate (2 L/min-8 L/min) were taken to investigate the photocatalytic performance of photocatalysts in fluidized bed reactor. The photocatalytic performance of the immobilized F-TiO_2 was compared with commercial Degussa P-25 in the phenol degradation.

The reaction kinetics parameters were further studied based on Langmuir-Hinshelwood kinetics model. The rate of reaction is determined based on initial phenol concentration as kinetic parameter in the photocatalytic degradation of phenol. Optimization and analysis of the operating parameters in the photocatalytic degradation of phenol were determined using response surface methodology (RSM). The selected operating parameters were initial phenol concentration, catalyst loading, and air flow rate.

1.6 Organization of Thesis

This thesis is made up of five chapters that cover important data regarding the research. Chapter 1 (Introduction) gives a brief description on the treatment of industrial effluent and heterogeneous photocatalysis. This chapter also includes problem statement, research objectives as well as the organization of the thesis.

Chapter 2 (Literature review) begins with the history of the photocatalysis. Advanced oxidation process and heterogeneous photocatalysis are accessed in detail. Next, the descriptions of TiO_2 as a photocatalyst, doping process, immobilization of TiO_2 onto support followed by reactor of photodegradation are discussed as they play important roles wherein the reaction takes place. Subsequently, the phenol photodegradation, characteristic of phenol, and process parameters such as catalyst loading (1 g/L-5 g/L), initial phenol concentration (10 mg/L-50 mg/L), metal cations (Zn^{2+}, Ca^{2+}, and K^{+} ions), inorganic anions (SO_4^{2-}, HCO_3^{-}, NO_3^{-} ions), and air flow rate (2 L/min-8 L/min) are embodied. Chapter 2 is ended with a short review of the design of experiment (DOE) including the response surface methodology (RSM).

Chapter 3 (Experimental) unveils the experimental part. Materials, equipment, and photocatalytic reactor used in this project are described. Meanwhile, the detailed of the synthesis and characterization of the prepared photocatalysts are studied throughout this research. The process parameters and optimization process are also included in this chapter.

Chapter 4 (Results and discussion) shows the results accompanied with discussions of the findings related to current research work. This chapter includes discussion of characterization results of suspended F-TiO_2 and immobilized F-TiO_2, effect of synthesis parameters of F-TiO_2 (hydrothermal treatment duration and

amount of fluoride doped), preliminary studies, effect of the operating parameters on the photocatalytic degradation of aqueous phenol solution in a fluidized bed reactor using suspended F-TiO_2 and immobilized F-TiO_2, comparison photocatalytic activity between immobilized F-TiO_2 and commercial Degussa P-25, optimization studies using RSM, and reaction kinetic studies from the Langmuir-Hinshelwood kinetic model representing the degradation rate of phenol over different concentrations.

Chapter 5 (Conclusion and recommendations) gives the overall conclusion based on the results obtained throughout the current study as previously discussed in Chapter 4. Some suggestions for future studies are also included as a continuation for the present one.

CHAPTER 2

LITERATURE REVIEW

This chapter reviews background information on the photocatalysis that leads to this research work. It begins with the wastewater treatment, heterogeneous photocatalysis, properties of phenol, TiO_2 photocatalysts and doped TiO_2 photocatalysts, photocatalyst support, photoreactors, and design of experiment.

2.1 Wastewater Treatment

Industrial effluents contain various types of pollutants such as volatile organic compounds (VOCs), heavy metals, and aromatic compounds which require tedious process to be removed. Among all these pollutants, aromatic compounds are the most toxic and carcinogenic pollutants as they pose a threat due to high toxicity and resistivity to be decomposed. Wastewater treatment is a process of removing contaminants from wastewater and household sewage, both industrial effluents and domestic. It includes physical, chemical, and biological processes to degrade and remove physical, chemical, and biological contaminants.

Several wastewater treatment techniques for the removal of organic pollutants include pre-treatment process, pre-sedimentation process (Björklund *et al.*, 2001), biological treatment (LaPara and Alleman, 1999), adsorption (Rani and Dahiya, 2008), and activated sludge process (Leivisk *et al.*, 2008). However, these techniques do not effectively remove the contaminants in wastewater. They are slow treatments because the complete biodegradation of contaminants needs several days or weeks. Moreover, at high contaminant concentrations, they also present some disadvantages during operation.

Conventional wastewater treatments are not suitable in removing and degrading the organic pollutants because mostly the aromatic rings in the organic pollutants are physically and chemically stable, hence, the degradation process using conventional wastewater treatments is normally selective and incomplete. In this way, efficient, environmentally benign, and low cost approaches for the degradation and removal of organic pollutants have been focused of current research to control the water quality.

2.2 Advanced Oxidation Process

Advanced oxidation process (AOP) is a process to treat the organic pollutants, which usually have high chemical stability or low biodegradability. It is normally used in treating the organic pollutants which are not treatable by the conventional techniques (Oller *et al*., 2010). It has been singled out as a particularly attractive in oxidizing and decomposing toxic organic pollutants, including carcinogenic chemicals, from industrial wastewater. The contaminants are chemically transformed to simpler or harmless compounds.

In general, AOP involves two stages of the oxidation, which are (1) the formation of strong oxidizing species (hydroxyl radical, •OH) and (2) the reaction of the oxidizing species with the organic pollutant. The hydroxyl radicals act very rapidly with most of organic compounds due to their powerful, non-selective oxidizing agents (Amat *et al*., 2007). •OH are used to degrade the organic pollutants by attacking the electron-rich site of the organic compounds and breaking the aromatic rings to carbon chain compounds, and hence, further mineralizing the carbon chain compounds to harmless products (carbon dioxide and water) (Galindo *et al*., 2000).

Commonly, the generation of hydroxyl radicals is accelerated by other strong oxidizing reagents such as hydrogen peroxide (H_2O_2) or ozone (O_3) or combining them with catalyst (TiO_2) or radiation (ultraviolet (UV), visible, ultrasonic, or electron-beam) in order to increase the efficiency of the organic pollutant removal (Lafi *et al*., 2009). In this study, only heterogeneous photocatalysis (UV/TiO_2) will be studied. TiO_2 catalyst is chosen due to its unique characteristics such as non-expensive, effective, and solid phase (Amat *et al*., 2007).

2.3 Photocatalysis

Photocatalysis is a series of reactions in the presence of a semiconductor (known as a catalyst). When the energy is greater than band gap energy of TiO_2 photocatalyst, free electrons are excited and transferred from valence band to conduction band, while positive holes remain in the valence band (Robert and Malato, 2002). These photogenerated electron-hole pairs are applied in the redox reaction through the formation of adsorbed radicals on the surface of TiO_2 photocatalysts (Jiang *et. al*., 2004). Titanium dioxide (TiO_2) is one of the most common photocatalyst used in photocatalytic process (Grzechulska-Damszel *et al*., 2009). A general brief scheme of the photocatalysis process can be summarized as follow (Robert and Malato, 2002):

$$TiO_2 + h_v \longrightarrow e_{cb}^- + h_{vb}^+ \qquad \text{Equation 2.1}$$

where h_v is energy required to transfer the excited electron, e_{cb}^- from the valence band to the empty conduction band and energized positive holes, h_{vb}^+.

In this reaction, the electron and positive hole generated will recombine or separate by the electrical field which generated at solid side of the semiconductor

junction. The positive hole and electron are known as powerful oxidizing and reducing agents respectively. Generally, the positive hole reacts with either surface-bound water (H_2O) or pollutant to produce •OH (Puma *et al*., 2008).

$h_{vb}^{+} + H_2O \rightarrow \bullet OH + H^{+}$ Equation 2.2

$h_{vb}^{+} + OH^{-} \rightarrow \bullet OH_{ad}$ Equation 2.3

Meanwhile the positive hole can react directly with the polluting species (R_{ads}) to form R^{+} ions as shown in Equation 2.4.

$h_{vb}^{+} + R_{ads} \longrightarrow R^{+}$ Equation 2.4

On the other hand, the photogenerated electron in the conduction band reacts with an electron acceptor such as oxygen to produce superoxide radical anion ($O_2\bullet^{-}$) in the water.

$e_{cb}^{-} + O_2 \rightarrow O_2^{\bullet -}$ Equation 2.5

Basically, the oxidative and reductive reactions do not occur concurrently. Hence, when an accretion of electron occurs in the conduction band, the electron is then recombined with the positive hole in the absence of the photocatalyst. As the photocatalytic reaction proceeds in preference to the positive hole-electron recombining, efficient electron consumption is hence essential to promote the photocatalytic oxidation. The equation of the recombination of positive hole and electron is shown below:

$e_{cb}^{-} + h_{vb}^{+} \rightarrow TiO_2$ Equation 2.6

Thus, the organic pollutant (R_{ads}) is oxidized to form salts, carbon dioxide and water in the complete photocatalytic oxidation process.

$\bullet OH + R_{ads} + O_2 \rightarrow$ products (salts, CO_2, H_2O) Equation 2.7

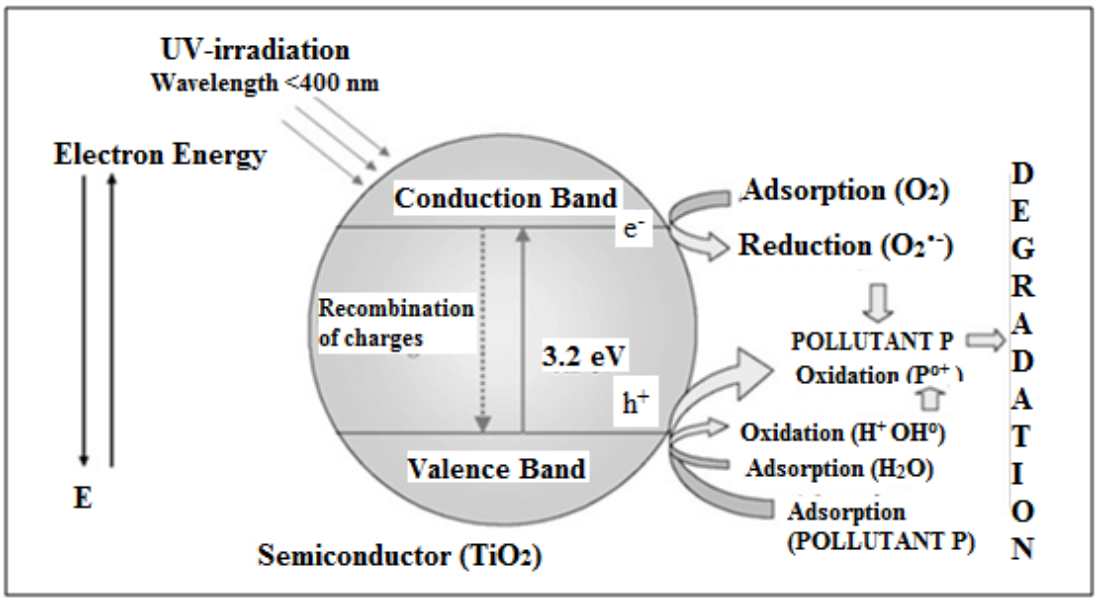

Figure 2.1 Schematic Representation Diagram of Photocatalysis Reaction upon Irradiation of TiO_2 (Herrmann, 2010).

2.4 Phenol

Phenol is an organic compound with its chemical formula C_6H_5OH. Phenol appears as a white crystalline solid with a disinfectant smell at room temperature. It is noted that phenol has low melting point and high boiling point of 42 °C and 182 °C respectively. It is also a weak acid due to its hydroxyl (OH) group.

Phenol is produced in the industrial scale annually as it is functional precursor to a large collection of many materials (Weber, 2004), such as cosmetics, plastics, reagents in research laboratories, bisphenol A, and disinfectants in household cleaners. Currently, more than 90 % of phenol is manufactured using benzene and propylene via cumene process (Schmidt, 2005). Phenol is widely used in the industrial processes such as oil refineries, petrochemical plants, and phenolic resin industries (Cai *et al*., 2007). Due to its moderate solubility in water (about 8 g of phenol will dissolve in 100 g of water) and bioaccumulation, highly toxicity,

carcinogenicity, and causticity of the phenol can cause considerable adverse effects on the human health and aquatic ecosystems (Chemguide, 2004).

Inappropriate disposal of phenols in wastewater effluents from many industrial processes has attracted concerns since phenols pose a significant threat to the environment and human health. Studies showed that low concentration of phenol could harm the human cells and even bring death to the cells in the presence of high phenol concentration (McCall *et al*., 2009). Hence, US Environmental Protection Agency (USEPA) has set a limit of 0.5 mg/L of phenol in waters to human health during the phenol exposure from the possible harmful effects by drinking water or eating contaminated water plants and animals (Adam *et al*., 2010). In Malaysia, the limit of phenolic compounds in raw drinking water is 0.002 mg/L (WEPA, 2011), while the maximum acceptable limit of phenolic compounds in wastewater emissions for sewage and industrial effluents are in the range of 1-5 mg/L (Abdullah et al., 2007).

Furthermore, phenol can be degraded to harmless products (carbon dioxide and water) via photocatalytic degradation process. Many studies have been done in photodegradation of phenol using TiO_2 photocatalysts (Marc *et al*., 1995; Lam *et al.,* 2010; Mantilla *et al*., 2010; Sin *et al.,* 2010; Zainudin *et al.,* 2010).

Lam *et al.* (2010) studied the photocatalytic degradation of phenol using TiO_2-P25/AC photocatalyst in the fluidized bed reactor. The TiO_2-P25/AC exhibited higher photocatalytic activity than that of the commercial Degussa P25 due to the presence of P25. The photocatalytic ability of TiO_2-P25/AC was reduced only 10 % after five cycles for phenol degradation.

Zainudin *et al.* (2010) studied the SNTZS photocatalyst synthesis and photocatalytic degradation of phenol in batch reactor. High crystalline quality, large specific surface area, low electron–hole pairs recombination rate, and small particle size of SNTZS enhanced its photocatalytic activity in the phenol degradation.

2.5 TiO_2 Photocatalysis

The basis of photocatalyst is the photo-excitation of a semiconductor that is solid as a result of the absorption of electromagnetic radiation, often, but not exclusively, in the near UV spectrum. TiO_2 (Fu *et al.*, 2004), $BiVO_4$ (Kudo, 2006), and Cu_2WS_4 (Jing *et al.*, 2010), etc can be used as photocatalysts. Among these photocatalysts, TiO_2 is a very well known photocatalyst owing to its idealistic, photo stability, chemically and biologically inert, low cost, and high availability and capability to adsorb reactants under efficient photonic activation (Gaya and Abdullah, 2008). They have many advanced functions in catalysis, gas sensors, photocatalysis, self-cleaning panels, solar energy cells, and photovoltaic cells (Tian *et al.*, 2008). The photocatalytic property has been known to have a mutual effect between the two determining factors: photocatalysis and photo-induced super-hydrophilicity (Fujishima *et al.*, 2007).

The discovery of TiO_2 by Fujishima and Honda (Chen and Mao, 2007) in 1972 opened new field in photocatalytic splitting of water. The extensive work has been carried out to produce hydrogen from the water by this novel oxidation/reduction reaction using a variety of semiconductors. Otherwise, interest has been focused on the use of semiconductors as photocatalysts in the heterogeneous photocatalysis (Fujishima and Zhang, 2006).

Nanostructured TiO_2 such as nanowires, nanopowders (Chung *et al.*, 2008), nanorods (Zhao *et al.*, 2007), and nanotubes (Yu *et al.*, 2007) present new opportunities and features for improved performance in the photocatalysis. There are several crystalline phases of TiO_2 and it usually exists in two forms: anatase and rutile which have the band gap value of 3.2 eV and 3.0 eV respectively. Anatase type of TiO_2 exhibits the photocatalytically most active modification of TiO_2 owing to its high band gap, thus, it acts as a catalyst or photocatalyst (Puma *et al.*, 2008). In the photocatalysis process, TiO_2 is photo-activated under UV irradiation and a redox reaction is then generated, which lead to the degradation of the organic pollutants.

2.6 Synthesis of TiO_2

There are many methods of the TiO_2 synthesis that can be used in the photocatalytic studies nowadays. The synthesis of TiO_2 can be briefly classified into 6 types, simple hydrolysis method (Vats *et al*., 2010), sol gel treatment (Eremenko *et al.*, 2000), hydrothermal technique (Lee *et al.*, 2004), solvothermal treatment (Zhang *et al.*, 2010a), sonoelectrochemical method (Liu *et al.*, 2004), and deposition-precipitation method (Wu *et al.*, 2010). Notwithstanding the methods mentioned above, hydrothermal method is chosen to prepare TiO_2 catalysts in this study because of its many advantages like high surface area, small particle size, high stability, and excellent photocatalytic activity (Kang *et al.*, 2003; Jing *et al.*, 2011).

Hydrothermal method is known as a low temperature technology, which usually carried out in a steel pressure vessel at elevated temperature and pressure. It is also defined as heterogeneous chemical reaction, which takes place in an aqueous solution within a closed system, using water as the reaction medium (Byrappa and Adschiri, 2007). Hydrothermal method is widely applied in the production of TiO_2

because of its many advantages, such as the requirement of low temperature and energy, simple equipment requirement, environmentally friendly chemicals, large capacity of crystals growth, superior crystal structure, and low concentrations of impurities (Liu *et al.*, 2005; Dem'yanets and Lyutin, 2008). Otherwise, hydrothermal reaction can easily manipulate the structure and skeleton of the catalysts by changing the surface area, particle size, and porous structure of the catalysts (Leboda *et al.*, 1995). Moreover, hydrothermal reaction also allows for the manipulation of large number of variable factors by which the surface morphology, grain size, crystalline phase, and surface chemistry of the particle produced is controlled (Kontos *et al.,* 2005).

Many researchers investigated their studies on the formation of TiO_2 using hydrothermal method (Wang and Kang, 2004; Kontos *et al.,* 2005; Jin *et al.,* 2009a; Tian *et al.,* 2009; Zhang *et al.,* 2010a; Huang *et al.,* 2011; Jing *et al.,* 2011). For example, Wang and Kang (2004) successfully produced TiO_2 nanoparticles of 10 nm diameter using hydrothermal method. Similarly, Jin *et al.* (2009a) used a simple hydrothermal process to produce TiO_2 of about 10 nm diameters with 150-192 m^2/g specific surface area. Single anatase of non-agglomerated TiO_2 with good crystalline phase, small crystalline size, and large surface area was successfully synthesised by Jing *et al.* (2011) via hydrothermal process. Zhang *et al.* (2010a) successfully produced TiO_2 of tri-phase (anatase, rutile, and brookite), bi-phase (anatase and rutile), and pure rutile TiO_2 nanoparticles using hydrothermal method. Tian *et al.* (2009) reported that the hydrothermal treatment was necessary for the formation of mesoporous TiO_2 of 30 nm diameter at 180 °C. In 2011, Huang and his workers found that pure anatase phase TiO_2 of 5.0-8.6 nm crystalline size were formed using

hydrothermal method beyond the hydrothermal temperature of 150 °C (Huang *et al.,* 2011).

Meanwhile, many researchers investigated their studies on the photocatalytic degradation processes using TiO_2 formed by hydrothermal method (Kim and Kwak, 2007; Jin *et al.,* 2009a; Jin *et al.,* 2011). For instance, Jin *et al.* (2009a) studied the photocatalytic activity of TiO_2 produced using hydrothermal treatment. They found that high photocatalytic activity of the produced TiO_2 compared to commercial Degussa P25 under UV irradiation. Jing and his workers (2011) investigated the photocatalytic degradation of dimethyl phthalate using TiO_2 produced by hydrothermal and sol gel processes. In their study, they found that TiO_2 produced using hydrothermal treatment showed 2.5 times higher photocatalytic activity as compared to TiO_2 produced by sol gel process. Kim and Kwak (2007) investigated the photocatalytic performance of mesoporous TiO_2 prepared by hydrothermal treatment on the degradation of methylene blue under UV irradiation. Their results showed that TiO_2 prepared by hydrothermal method exhibited much higher photocatalytic activity than commercial Degussa P25. Their results showed that the hydrothermal treatment should be compensated by the benefits of improving crystallinity, crystal composition, surface area, thermal stability, and pore size distribution.

Some researchers stated that the catalysts produced using traditional hydrothermal method could not aid the agglomeration problem (Wang and Kang, 2004; Liu *et al.,* 2010). Excessive duration of hydrothermal treatment could lead to a significant decrease in the specific surface area and hydroxyl content of particle which eventually impede the efficiency of photocatalytic activity (Kontos *et al.*, 2005). Thus, the modification of the traditional hydrothermal method is applied, such

as microwave-assisted hydrothermal (Huang *et al.*, 2010), ultrasonic-assisted hydrothermal (Meskin *et al.*, 2006), or sonication-assisted hydrothermal (Viriya-empikul *et al.*, 2009).

In this master study, sonication-assisted hydrothermal method is applied to produce TiO_2 catalyst. The sonication pre-treatment of TiO_2 synthesis is proven that it can improve the physical properties of TiO_2 produced (Viriya-empikul *et al.*, 2009). Zhu *et al.* (Ou and Lo, 2007) have proposed a sonication-assisted hydrothermal treatment in which the synthesis time is shortened from 20 h to 4 h. This is based on chemical effect of sonication treatment from acoustic cavitations, that is, the formation, growth, and collapse of bubbles in liquid medium (Yu *et al.*, 2009a). The implosive collapse generates high temperatures and pressures with localized hot spots, characterized by transient temperatures (>5000 K) and pressures (>1800 atm). TiO_2 nanoparticles showing a more controlled phase composition, a more uniform size distribution, higher surface area, are some of the important properties resulting from the application of sonication-assisted hydrothermal method (Cappelletti *et al.,* 2009).

2.7 Doping techniques

TiO_2 is a well known photocatalyst that is not only sensitive to light and corrosion resistant, but also inexpensive as an industrial material (Nowotny *et al.*, 2007). However, there are disadvantages linked to the use of TiO_2 as a photocatalyst. These include the wide band gap, ineffectiveness of photocatalysis under sunlight, thermal instability (Zhang *et al.*, 2009; Kim *et al.*, 2010), the difficulty in producing high grade TiO_2 with tightly controlled physical properties and the fact that, in its basic form, it functions only under UV irradiation (Rengifo-Herrera *et al.*, 2009).

Many factors govern the physical-chemical properties of TiO_2 during its production such as the speed of growth, the diffusion coefficient, and the ionic radii (Carvajal *et al.*, 2002). The methods of synthesis and post treatment conditions also play prominent roles in synthesizing a high efficiency TiO_2 product (Supphasrirongjaroen *et al.*, 2008). To overcome some of the difficulties encountered, doping techniques have been applied to photocatalysts to overcome the limitations of nano-TiO_2 with the aims of enhancing the morphology and photocatalytic activity of TiO_2 in the photocatalysis (Carp *et al.*, 2004).

Basically, nano-TiO_2 can only utilize 6 % of the total solar irradiation in photocatalysis due to the large band gap of anatase nano-TiO_2 (3.2 eV), but doping techniques shift the activity of nano-doped-TiO_2 from the UV region to the visible light region (Zhang *et al.*, 2009). Dopants modify the electronic structure of TiO_2 to broaden its effective range of light sensitivity for photocatalysis from the ultra-violet (UV) region to the visible light region (Kudo *et al.*, 2007). Doping techniques have been shown to be effective and efficient despite their being susceptible to thermal instability and their requirement for expensive ion-implantation facilities (Wang *et al.*, 2007). Dopants are valued for their ability to confer excellent physicochemical properties such as high crystallinity (high percentage of anatase phase), high specific surface area, and small crystallite size (Fan *et al.*, 2008; Setiawati and Kawano, 2008). The formation of the anatase and rutile phases or phase transformation from anatase to rutile is strongly dependent on the formation of the Ti-O-Ti bonds by the interaction between -OH groups and the protonated surfaces during thermal dehydration process. The phase transformation from anatase to rutile occurs when the thermal energy is high enough to overcome the nucleation barrier during the thermal dehydration process, and this occurs more readily with the larger crystallite

size of TiO_2. Dopants suppress the crystallite size of TiO_2 by inserting itself into the lattice structure of the TiO_2 octahedral to modify its physicochemical properties.

Specific surface area of TiO_2 is one of the factors that determine the morphology of TiO_2 in photocatalysis. A large specific surface area of TiO_2 enhances the photocatalytic degradation rate of organic pollutants as availability of active sites in TiO_2 is increased (Liu *et al.,* 2006; Kim *et al.,* 2007). Crystallite size is another important characteristic that determines the quality of TiO_2. The performance of nano-TiO_2 can be enhanced in the photocatalysis by producing nano-doped-TiO_2 with high crystallite size up to a certain limit (Kongsuebchart *et al.,* 2006). Thereafter, the photocatalytic performance of nano-doped-TiO_2 decreases when the crystallite size falls beyond this limit because of the trapping of charge carriers during the diffusion process. With the presence of dopants in the formation of nano-doped-TiO_2, the phase transformation from anatase to rutile inhibits when the thermal energy is low enough to overcome the nucleation barrier during the thermal dehydration process, and this occurs more readily with the smaller crystallite size of nano-doped-TiO_2 (Hirano *et al.,* 2003). In short, dopants suppress the crystallite size of nano-TiO_2 by inserting itself into the lattice structure of the nano-doped-TiO_2 octahedral to modify its physicochemical properties. In general, a smaller crystallite size of nano-doped-TiO_2 is favoured compared to larger crystallite size of nano-doped-TiO_2 since the smaller size reduces the recombination of the photogenerated charge carriers (Devi *et al.,* 2010). Some researchers reported that smaller crystallite size of nano-doped-TiO_2 induced a larger band gap due to the increased redox ability (Kim *et al.,* 2007). The resultant photocatalytic activity benefits from the quantum size effect of nano-doped-TiO_2 that enhances its photocatalytic activity (Liu *et al.,* 2006).

Although nano-doped-TiO_2 with large specific surface area, high percentage of anatase phase, and small crystallite size all contribute towards high photocatalytic activity, a complete understanding of the inter-linkages between these variables has yet to be achieved and their detailed underlying mechanisms remain a challenge to researchers.

2.7.1 Effect of Metal Doping on the Formation of Nano-doped-TiO_2

Metal dopants have been used to improve the physical properties and photocatalytic activity of nano-doped-TiO_2. In previous studies, various metal dopants, including cobalt (Co) (Suriye *et al.,* 2005; Hsieh *et al.,* 2009), barium (Ba) (Atashfaraz *et al.,* 2007), manganese (Mn) (Zhang *et al.,* 2006b), nickel (Ni) (Wang *et al.,* 2004), copper (Cu) (Chen *et al.,* 2009), zinc (Zn) (Xu *et al.,* 2005), and iron (Fe) (Janes *et al.,* 2004; Deng *et al.,* 2009), have been analyzed for their abilities to enhance the photocatalytic performance of nano-doped-TiO_2. They improve nano-doped-TiO_2 performance under visible light irradiation by shifting the absorption spectra to a lower energy region (Tsai and Teng, 2008). In addition, various approaches have been attempted to sustain photocatalytic activity by limiting the recombination of the photogenerated electron-hole pairs in photocatalysis.

Hsieh *et al.* (2009) produced Co-doped titania nanotubes with a specific surface area of 379 m^2/g, outer diameter of 10-15 nm, and inner diameter of 5-10 nm. Suriye *et al.* (2005) found that Co-doped TiO_2 exhibited high anatase phase based on X-ray diffraction (XRD) patterns. Smaller particle size of Ba-doped TiO_2 were synthesized by Atashfaraz *et al.* (2007) who reacted TiO_2 and barium hydroxide at high temperature in the flow reactor. Zhang *et al.* (2006b) produced Mn-doped TiO_2 using the sol gel method. Based on their observations, the band gap of the

photocatalyst was narrowed due to the formation of an impurity level near the bottom of the conduction bands. Xu *et al.* (2005) showed that Zn which was located on the titania nanotube surface had little effect on the titania nanotube morphology. Fe-doped titania prepared by Jane *et al.* (2004) using the sol gel method prevented the phase transformation of anatase to rutile at low dopant levels. The interaction was applicable to a maximum Fe dopant loading of 5.64 wt%. Deng *et al.* (2009) also investigated the morphology of Fe-doped titania nanotubes synthesized by the sol gel and hydrothermal methods. They found that the addition of Fe slowed the crystallization process and prevented the growth of crystallite TiO_2.

Besides metal dopants, transition metals dopants such as palladium (Pd), chromium (Cr), and silver (Ag) have been investigated by Wu *et al.* (2004) to enhance the photocatalytic performance of nano-doped-TiO_2. Among the transition metals dopants tested, Pd ion had the strongest interaction with nano-TiO_2 and improved its morphology most effectively. Some researchers are of the opinion that doping techniques promote the production of smaller crystallite nano-doped-TiO_2 with the resultant larger surface area helping to prevent the problem of particle agglomeration (Asiltürk *et al.,* 2009).

Sakthivel *et al.* (2004) investigated the performance of TiO_2 after supplementing with platinum (Pt) dopant. Pt acted as an electron trap in the formation of TiO_2, decreasing its surface area. While the generated free electrons gravitated towards Pt that served as a temporary electron trap preventing electron-energized hole recombination, increased Pt also competed with TiO_2 as an electron trap to decrease effective surface area in the latter. A further increase in Pt dopant might lead to the following possible consequences: (1) shortening of the charge carrier space distance (Sakthivel *et al.,* 2004), (2) recombination of free electron and

energized hole (Huang *et al.,* 2008), (3) agglomeration of Pt and TiO_2 (Huang *et al.,* 2008), and (4) decrease in the probability of oxygen being photo-adsorbed on TiO_2 (Sakthivel *et al.,* 2004). The crystallite size of 9.15-31.00 nm and a specific surface area of 19.1-118.7 m^2/g of TiO_2 was produced by loading Pt at the rate of 0.1-1.5 wt% (Abe *et al.,* 2006; Colón *et al.,* 2008; Huang *et al.,* 2008; Sun *et al.,* 2008).

Chromium (Cr), cerium (Ce), and vanadium (V) have also been used as dopants for TiO_2. The addition of vanadium (V) increases the surface area and porosity of TiO_2 (Bettinelli *et al.,* 2007). The advantages of Ce as dopants include: (1) decrease of the rate of crystallite growth, (2) promotion of mesoporous materials formation, (3) promotion of the stability of the active phase, (4) prevention of thermal loss in the catalyst area, and (5) prevention of the phase transformation of the anatase to the rutile phase (Xiao *et al.,* 2006).

Metal-doped TiO_2 products reveal the presence of the anatase phase and a crystallite size of TiO_2 ranging from 2.59-12.00 nm. The specific surface area of TiO_2 is in the region of 100-500 m^2/g (Sakthivel *et al.,* 2004; Zhu *et al.,* 2004; Xiao *et al.,* 2006; Bettinelli *et al.,* 2007; Hung *et al.,* 2007; Kozlova & Voronstov, 2007; Ambrus *et al.,* 2008; Colón *et al.,* 2008; Huang *et al.,* 2008; Ishibai *et al.,* 2008; Sun *et al.,* 2008; Tong *et al.,* 2008; Adán *et al.,* 2009; Asiltürk *et al.,* 2009; Wang *et al.,* 2010a). Table 2.1 which summarizes the dopants used in TiO_2 formation shows that different dopants are responsible for different structural properties of the TiO_2. Further studies are needed to understand the mechanism of metal doping in the formation of TiO_2 and the influence of metal dopants in its morphology.